



This is a repository copy of *Electrically pumped continuous-wave III–V quantum dot lasers on silicon*.

White Rose Research Online URL for this paper:  
<http://eprints.whiterose.ac.uk/111812/>

Version: Supplemental Material

---

**Article:**

Chen, S., Li, W., Wu, J. et al. (9 more authors) (2016) Electrically pumped continuous-wave III–V quantum dot lasers on silicon. *Nature Photonics*, 10. pp. 307-311. ISSN 1749-4885

<https://doi.org/10.1038/nphoton.2016.21>

---

**Reuse**

Unless indicated otherwise, fulltext items are protected by copyright with all rights reserved. The copyright exception in section 29 of the Copyright, Designs and Patents Act 1988 allows the making of a single copy solely for the purpose of non-commercial research or private study within the limits of fair dealing. The publisher or other rights-holder may allow further reproduction and re-use of this version - refer to the White Rose Research Online record for this item. Where records identify the publisher as the copyright holder, users can verify any specific terms of use on the publisher's website.

**Takedown**

If you consider content in White Rose Research Online to be in breach of UK law, please notify us by emailing [eprints@whiterose.ac.uk](mailto:eprints@whiterose.ac.uk) including the URL of the record and the reason for the withdrawal request.



[eprints@whiterose.ac.uk](mailto:eprints@whiterose.ac.uk)  
<https://eprints.whiterose.ac.uk/>

Supplementary Information:

## Electrically Pumped Long Lifetime Continuous-Wave III-V Quantum-Dot Lasers Directly Grown on Silicon Substrates

Siming Chen<sup>1\*</sup>, Wei Li<sup>2</sup>, Jiang Wu<sup>1</sup>, Qi Jiang<sup>1</sup>, Mingchu Tang<sup>1</sup>, Samuel Shutts<sup>3</sup>, Stella N. Elliott<sup>3</sup>, Angela Sobiesierski<sup>3</sup>, Alwyn Seeds<sup>1</sup>, Ian Ross<sup>2</sup>, Peter Smowton<sup>3</sup>, and Huiyun Liu<sup>1\*</sup>

### I. General wafer characterization

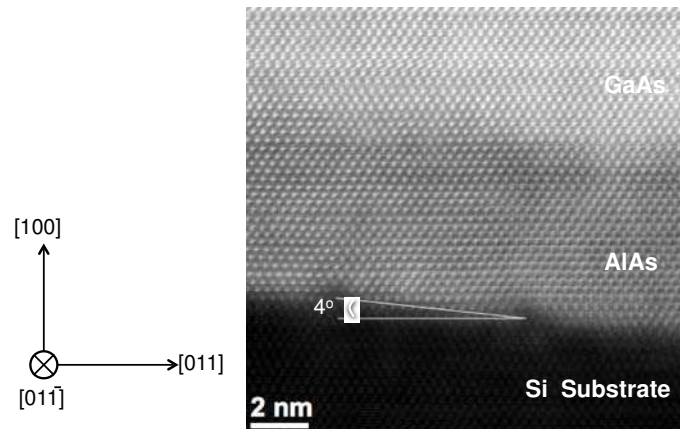


**Figure S1.** High-resolution high angle annular dark field scanning TEM image of interface, showing the offcut of silicon substrate is  $4^\circ$ .

High-resolution high angle annular dark field Z-contrast scanning TEM images allow direct atom-level interpretation of micrographs of AlAs/Si interface. The silicon substrate offcut  $4^\circ$  towards the  $[011]$  plane is typically characterized by a double silicon atom step to suppress anti-phase domains (APDs)<sup>1</sup>.

<sup>1</sup> Department of Electronic and Electrical Engineering, University College London, London WC1E 7JE, United Kingdom, <sup>2</sup> Department of Electronic and Electric engineering, University of Sheffield, Sheffield, S1 3JD, United Kingdom, <sup>3</sup> Department of Physics and Astronomy, Cardiff University, Queens Building, The Parade, Cardiff, CF24 3AA, United Kingdom. \*email: [siming.chen@ucl.ac.uk](mailto:siming.chen@ucl.ac.uk); [huiyun.liu@ucl.ac.uk](mailto:huiyun.liu@ucl.ac.uk)

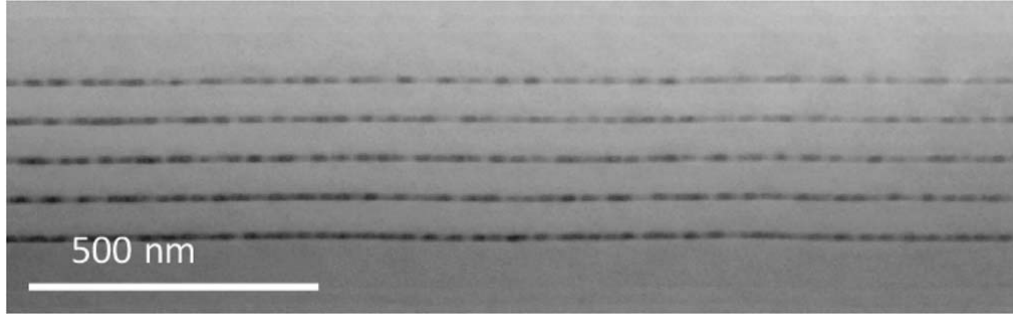


**Figure S2.** Bright field scanning TEM image of active region in low magnification.

Bright field scanning TEM measurements were also carried out on the laser active region under very low magnification showing no threading dislocations observed in active region over a large area.

## II. Uniformity of QD material grown on Si

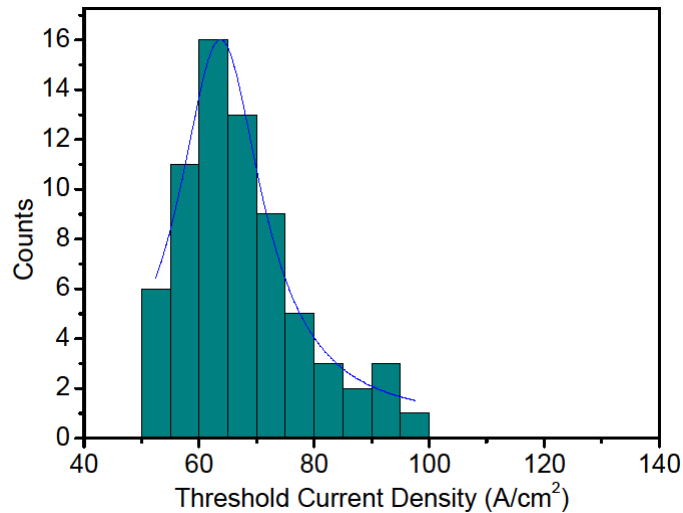


**Figure S3.** Histogram of threshold current density of QD lasers on silicon at room temperature under pulsed operation.

In order to achieve massively scalable and streamlined fabrication of QD based lasers on silicon, uniformity of QD material is an essential parameter. Here, to estimate the uniformity of QD material grown on Si, L-I characteristics have been carried out on 70 Si-based QD lasers (with the same cavity length of 3,200  $\mu\text{m}$ ), from different areas within a quarter 3-inch wafer, under pulsed operation (1% duty cycle and 1 $\mu\text{s}$  pulse width) at room temperature. A histogram of measured threshold current densities is presented, where a 90 % distribution of threshold current density of 67.5 +/- 17.5 A cm<sup>-2</sup> is obtained, indicating excellent uniformity of QD material.

### III. Images of III-V on silicon laser with as-cleaved facets

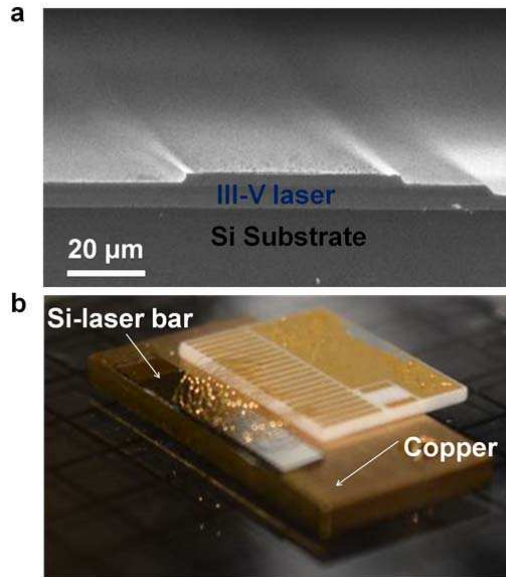


**Figure S4.** Fabricated III-V on silicon laser. (a) A SEM image of fabricated III-V laser on a Si substrate; (b) A picture of assembled Si-based laser bar mounted on copper with Au-wire bonded on the ridges.

As-cleaved laser bars were mounted on gold-plated copper heat sinks using indium-silver low melting point solder, which is not ideal for c.w. operation, especially for life-test measurement. Therefore, all the measurements in this work were performed as a feasibility study, and all the data presented represent worst case results.

### IV. General characterization of cleaved-facet QDs lasers grown on Si

#### LIV measurements for different cavity lengths at RT

LIV characteristics for 50 μm wide InAs/GaAs QD lasers grown on silicon substrates with 2670 μm and 3200 μm cavity lengths under c.w. operation at room temperature are compared. The measured series resistances extracted from IV curves are  $1.9 \pm 0.2 \Omega$  and  $1.8 \pm 0.2 \Omega$  for the 50 μm × 3200 μm and 50 μm × 2670 μm devices, respectively. The slope efficiency and external differential quantum efficiency (measured between 300 and 600mA) for the 50 × 3200 μm laser are 0.165 W/A and 17.5%, respectively. By shortening the cavity length to 2670 μm, the slope efficiency and external differential quantum efficiency are increased to 0.191 W/A and 20.3% respectively, owing to larger photon emission rate per increment of current, from lasers with shorter cavity lengths.

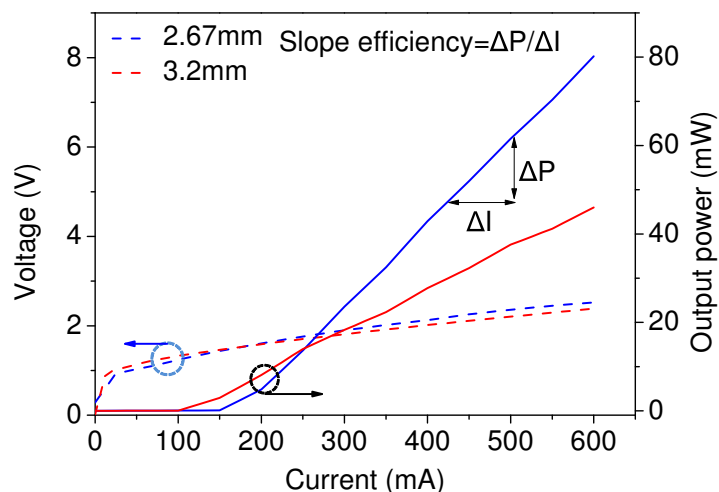


**Figure S5.** LIV characteristics for a  $50 \mu\text{m} \times 3200 \mu\text{m}$  and a  $50 \mu\text{m} \times 2670 \mu\text{m}$  InAs/GaAs QD lasers grown on silicon substrate under c.w. operation at room temperature.

#### Temperature-dependent lasing spectrum measurement

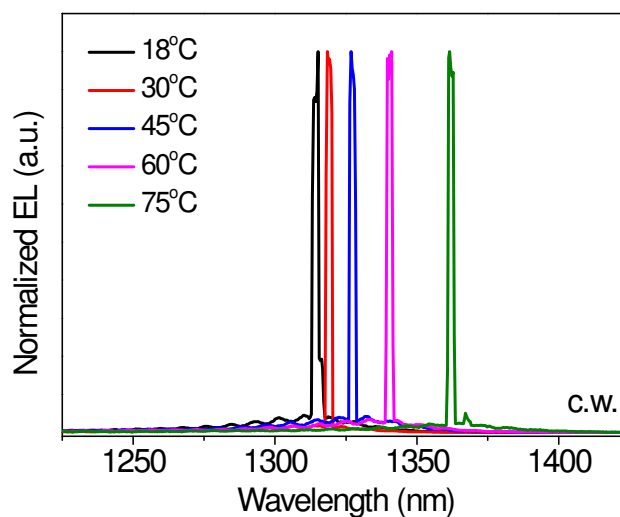


**Figure S6.** Lasing spectra measured 5% above the threshold at various heat sink temperatures under c.w. operation.

Lasing spectra for a  $50 \mu\text{m} \times 3200 \mu\text{m}$  InAs/GaAs QD laser grown on a silicon substrate measured 5% above the threshold at various heat-sink temperatures under c.w operation are shown. It is clearly seen that the c.w. lasing in the ground state is maintained up to a heat-sink temperature up of  $75^\circ\text{C}$ .

## Temperature-dependent LI and $T_0$

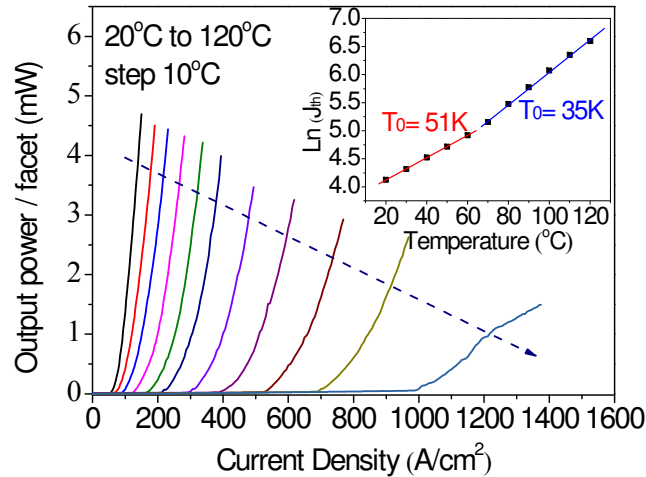


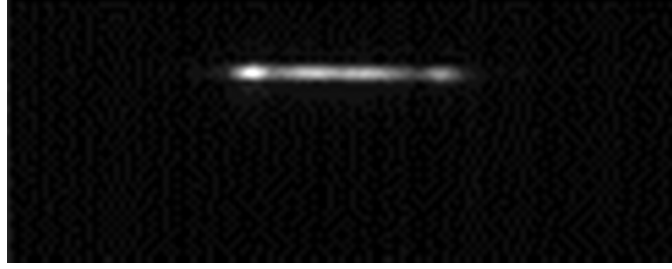
**Figure S7.** Light output power versus current density for a  $50 \mu\text{m} \times 3200 \mu\text{m}$  InAs/GaAs QD laser on silicon at various heat sink temperatures under pulsed operation. The inset shows the natural logarithm of current density,  $\ln(J_{\text{th}})$  against temperature, with the red and blue curves fitting data in the temperature ranges 20-60 °C and 70-120 °C, respectively.

Light output power versus current density for a  $50 \mu\text{m} \times 3200 \mu\text{m}$  InAs/GaAs QD laser on silicon is shown at various heat-sink temperatures under pulsed operation (1% duty-cycle and  $1 \mu\text{s}$  pulse-width). With limited self-heating, a maximum lasing temperature of 120 °C has been achieved. The characteristic temperature ( $T_0$ ) for this device estimated under pulsed operation is 51 K between 20 and 60 °C and 35 K between 70 and 120 °C. The majority of the effort towards further improving the maximum lasing temperature will be concerned with reducing the sensitivity of the laser to temperature and optimizing the extraction of heat from the active region. The well-established strategies to achieve this are modulation p-doping of the QDs<sup>2</sup> and mounting the laser diode epitaxial-side down on a high thermal conductivity heat-sink<sup>3</sup>.

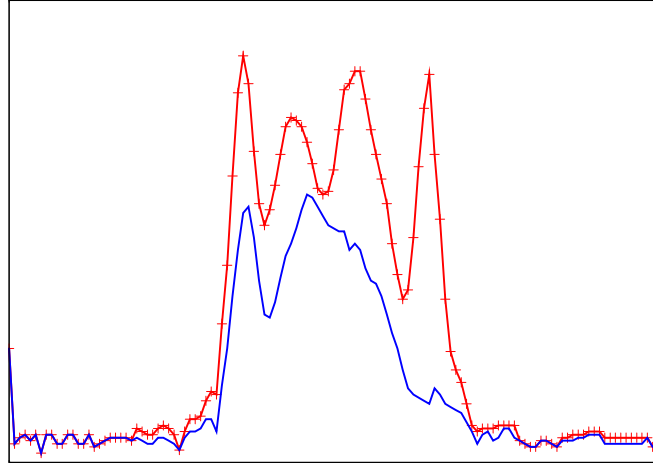
### Laser near-field measurements

We measured the spatial light emission characteristics of as-cleaved laser bars under a variety of pumping conditions. The devices were individually driven pulsed (1000 ns pulses at 1 kHz) at currents from 54 mA to 400 mA: well below to well above threshold. The nearfield emission was focused using a Mitutoyo M Plan Apo NIR 50x/0.42 lens on the CCD array of a Xeva 163 IR camera. The resulting images were analysed to obtain plots of intensity across the facet.

Faint light emission could be seen across the whole structure when operated below threshold giving confirmation of the width of the emission compared to the total structure width. This was also confirmed with supplementary measurements using an individual die from another set of samples. This faint emission could not be seen in the image below as the laser light had to be attenuated with neutral density filters above threshold to avoid saturating the camera.



(a)



(b)

**Figure S8.** Lasing near-field images, (a) Image of the lasing nearfield at 200 mA (well above threshold). (b) Intensity profile of the image in (a) (red line with markers) together with an intensity profile obtained at 150 mA (blue line without markers).

Figure S8(a) shows a camera image of the lasing nearfield well above threshold at 200 mA. It can be seen that light was emitted across the full width, with variations in intensity due to the lateral mode present. In Figure S8(b) the intensity profile of this image can be seen (red line with markers) together with an intensity profile obtained at 150 mA. It can be seen the mode order has changed as the pumping current increased which is to be expected in a broad area device.

## V. Estimating lifetime

A sub-linear model<sup>4,5</sup> shown below is employed to fit the measured threshold over time:

$$I_{th}(t) = I_{th}(0) (1 + at^m) \quad (1)$$

$$MTTF = (1/a)^{1/m} \quad (2)$$

where  $t$  is the elapsed aging time and  $I_{th}(t)$  is the threshold as a function of ageing time. The lifetime is defined as the time when the threshold current is doubled for consistency with

other reliability studies of lasers on Si. Figure S9 shows the ageing data. The red line is the best-fit curve for the measured threshold, from which an estimated lifetime of 100,158 hours is extrapolated.

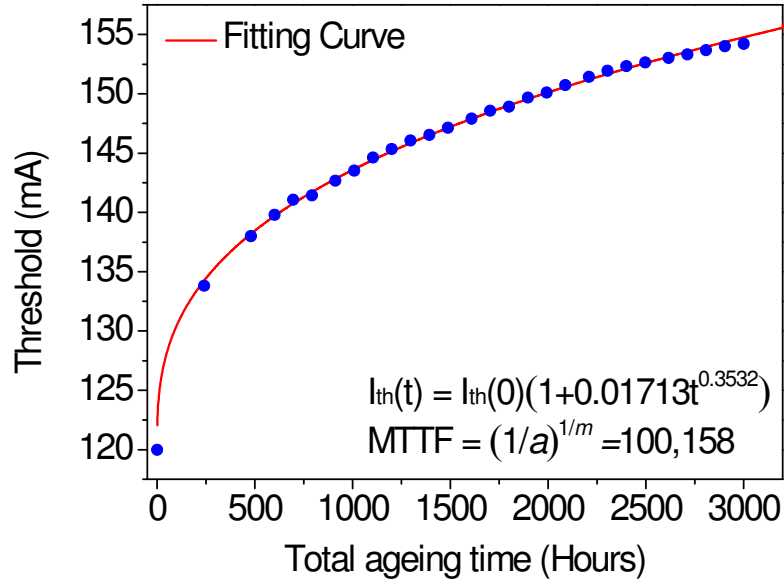


**Figure S9.** Ageing characteristic for QD laser grown directly on Si. The blue dots are the measured threshold currents and the red line shows the best-fit curve for the measured threshold current.

**Reference:**

1. R. Fischer *et al.*, Growth and properties of GaAs/AlGaAs on nonpolar substrates using molecular beam epitaxy. *J. Appl. Phys.* **58**, 374–381 (1985)
2. M. Sugawara, M. Usami, Quantum dot devices: Handling the heat. *Nat. Photonics* **3**, 30-31 (2009).
3. X. Li *et al.*, Improved continuous-wave performance of two-section quantum-dot superluminescent diodes by using epi-down mounting process. *IEEE Photon. Techn. Lett.* **24**, 1188-1190 (2012).
4. A. Liu *et al.*, Reliability of InAs/GaAs quantum dot lasers epitaxially grown on silicon. *IEEE J. Sel. Topics Quantum Electron.* **21**, 1900708 (2015)
5. S. Srinivasan *et al.*, Reliability of hybrid silicon distributed feedback lasers. *IEEE J. Sel. Topics Quantum Electron.* **19**, 1501305 (2013).